Available online at www.sciencedirect.com
SCIENCE DIRECT®
ELSEVIER
Earth and Planetary Science Letters 240 (2005) 495–509
EPSL
www.elsevier.com/locate/epsl

The Upper Valanginian (Early Cretaceous) positive carbon–isotope event recorded in terrestrial plants

Darren R. Gröcke [a,*], Gregory D. Price [b], Stuart A. Robinson [c], Evgenij Y. Baraboshkin [d], Jörg Mutterlose [e], Alastair H. Ruffell [f]

[a] *School of Geography and Earth Sciences, McMaster University, 1280 Main Street West, Hamilton, Ontario, Canada L8S 4K1*
[b] *School of Earth, Ocean and Environmental Sciences, The University of Plymouth, Drake Circus, Plymouth PL4 8AA, England, UK*
[c] *School of Human and Environmental Sciences, University of Reading, Whiteknights, PO Box 227, Reading RG6 6AB, England, UK*
[d] *Lomonosov State University, Department of Historical and Regional Geology, Vorobjovy Gory, Moscow 199899, Russia Moscow State University, Moscow, Russia*
[e] *Institut für Geologie, Mineralogie und Geophysik, Ruhr-Universität Bochum, Universitätsstraße 150, D-44801, Bochum, Germany*
[f] *School of Geography, Queen's University, Belfast, Northern Ireland, BT7 1NN, UK*

Received 30 July 2004; received in revised form 7 July 2005; accepted 26 August 2005
Available online 20 October 2005
Editor: E. Boyle

Abstract

Our understanding of the ancient ocean-atmosphere system has focused on oceanic proxies. However, the study of terrestrial proxies is equally necessary to constrain our understanding of ancient climates and linkages between the terrestrial and oceanic carbon reservoirs. We have analyzed carbon–isotope ratios from fossil plant material through the Valanginian and Lower Hauterivian from a shallow-marine, ammonite-constrained succession in the Crimean Peninsula of the southern Ukraine in order to determine if the Upper Valanginian positive carbon–isotope excursion is expressed in the atmosphere. $\delta^{13}C_{plant}$ values fluctuate around −23‰ to −22‰ for the Valanginian–Hauterivian, except during the Upper Valanginian where $\delta^{13}C_{plant}$ values record a positive excursion to ∼−18‰. Based upon ammonite biostratigraphy from Crimea, and in conjunction with a composite Tethyan marine $\delta^{13}C_{carb}$ curve, several conclusions can be drawn: (1) the $\delta^{13}C_{plant}$ record indicates that the atmospheric carbon reservoir was affected; (2) the defined ammonite correlations between Europe and Crimea are synchronous; and (3) a change in photosynthetic carbon–isotope fractionation, caused by a decrease in atmospheric pCO_2, occurred during the Upper Valanginian positive $\delta^{13}C$ excursion. Our new data, combined with other paleoenvironmental and paleoclimatic information, indicate that the Upper Valanginian was a cool period (icehouse) and highlights that the Cretaceous period was interrupted by periods of cooling and was not an equable climate as previously thought.

Keywords: carbon isotopes; plants; CO_2; icehouse; OAE; Valanginian; Early Cretaceous

1. Introduction

It has been suggested that the Valanginian period represents the first episode of Cretaceous greenhouse conditions with high paleoatmospheric pCO_2 levels [1]. These greenhouse conditions have subsequently

* Corresponding author.
E-mail addresses: grocke@mcmaster.ca (D.R. Gröcke), g.price@plymouth.ac.uk (G.D. Price), s.a.robinson@reading.ac.uk (S.A. Robinson), barabosh@geol.msu.ru (E.Y. Baraboshkin), joerg.mutterlose@ruhr-uni-bochum.de (J. Mutterlose), a.ruffell@qub.ac.uk (A.H. Ruffell).

0012-821X/$ - see front matter © 2005 Elsevier B.V. All rights reserved.
doi:10.1016/j.epsl.2005.09.001

been related to Valanginian carbonate-platform drowning episodes [2]. The Paraná-Etendeka continental flood basalts, which initiated at ~137 Ma during the latest Valanginian, may have been a source for CO_2 in the Early Cretaceous [3,4]. However, Courtillot et al. [4] report that volcanic activity did not peak until 133–131 Ma during the Upper Hauterivian [5] suggesting a trend towards increasing atmospheric pCO_2 levels during the Valanginian–Hauterivian. Geochemical models indicate that CO_2 levels were relatively steady through the Berriasian–Hauterivian [6,7], although Tajika [8] suggests a peak in pCO_2 at the Berriasian/Valanginian boundary. More recently, moderately low pCO_2 levels for the Early Cretaceous have been demonstrated through carbon–isotope data from soil carbonate nodules in the Lower Barremian (~560 ppm V; [9]) that supports the model results from Wallmann [6]. Seawater strontium–isotope data [10–15] indicate that there was a reduction in sea-floor spreading and/or increase in continental weathering from the Late Jurassic to mid-Cretaceous, both of which are conducive to an overall reduction in paleoatmospheric pCO_2 concentrations.

1.1. Was there a Late Valanginian Greenhouse event?

Recently, the greenhouse hypothesis for the Early Cretaceous, as proposed by Lini et al. [1], has been questioned. $\delta^{18}O_{carb}$ data from Valanginian and Hauterivian belemnites tend to suggest cooler conditions compared to data from earlier and later time periods [12,15–17]. This is supported by Valanginian paleotemperatures based on belemnites corrected for δ_w using ikaite in the Eromanga Basin, Australia [18,19]. Ditchfield [20] analyzed belemnites from Spitsbergen that record high $\delta^{18}O_{carb}$ values (i.e., low paleotemperatures) for the lower to middle Valanginian, indicating the presence of high latitude ice.

In further support of a cool episode, nannofossil data from localities throughout Europe indicate that the Late Valanginian–Early Hauterivian time period records cool (icehouse) conditions [21,22]. Glendonite carbonate nodules have also been taken to reflect cold sub-aqueous depositional conditions within Mesozoic successions [23–25]. In particular, widespread glendonites of Early Cretaceous (Valanginian) age have been described from the Sverdrup Basin of Canada [23,26], Spitsbergen [26], Siberia in the Taymyr Peninsular eastwards to the Lena River [27], and northern Alaska [28]. Recently, the discovery of a Berriasian–Valanginian tillite in South Australia provides the first direct evidence of a Cretaceous glaciation [29]. Within these successions outsized clasts also occur which have been attributed to ice rafting [24,30,31].

Stoll and Schrag [32] inferred the presence of pulsating Valanginian ice-sheets on the basis of high-resolution $\delta^{18}O_{carb}$ data from Deep Sea Drilling Project sites with a cyclicity of 250–500 kyrs. More recently Frank et al. [33] have shown that the changes in $\delta^{18}O_{carb}$ of bulk carbonate tend to be of diagenetic origin and not a reflection of paleoenvironmental changes, although this is still a matter of debate [34].

1.2. Valanginian $\delta^{13}C$ record and black shales

Bulk-marine carbonate carbon–isotope ($\delta^{13}C_{carb}$) records for the Early Cretaceous from northern Italy, France and Switzerland all indicate the presence of a positive carbon–isotope excursion in the Upper Valanginian [1,2,35–38]. A period of relatively stable $\delta^{13}C_{carb}$ values in the Lower Valanginian is followed by a rapid excursion to more positive values in the Upper Valanginian, with a subsequent return to pre-excursion values in the Lower Hauterivian.

Positive oceanic $\delta^{13}C_{carb}$ excursions have typically been explained by increased marine productivity, elevated carbon burial rates (resulting in the formation of 'black shales') and thus removal of ^{12}C from the exchangeable carbon reservoir [39–42]. However, evidence for widespread marine organic-rich black shales within the Valanginian is somewhat limited. DSDP Site 535 contains appreciable amounts of marine derived organic matter [43], which are coincident with the Valanginian positive carbon–isotope excursion [1]. More recently, ODP Leg 198 (Shatsky Rise, northwest Pacific Ocean) recovered pelagic successions containing two Valanginian-age organic-rich intervals of marine origin at Site 1213 [44]. Several ODP and DSDP sites in the Atlantic do contain organic-rich horizons of Valanginian age (e.g., Sites 416, 638), however, the organic matter is dominantly terrestrial in origin [45]. Similarly, amorphous organic matter and continental organic matter dominate Tethyan sections during the Late Valanginian, with only a minor component originating from marine phytoplankton [46].

Carbon–isotope investigations have shown that pelagic black-shale deposition does not necessarily coincide with positive excursions [47,48]. Coupled changes in the flux of marine and terrestrial organic and carbonate carbon may contribute to excursions in the carbon–isotope record of the global carbon reservoir [37,49]. The $\delta^{13}C_{org}$ record for the Valanginian has been documented in Tethyan marine carbonate sequences by Lini et al. [1] and in the Atlantic by

Wortmann and Weissert [50] at DSDP Site 416 (offshore Morocco). However, in both studies, the nature of the organic matter (terrestrial versus marine) was not determined and this may explain some of the scatter observed in the carbon–isotope data.

1.3. Terrestrial $\delta^{13}C$ curves: correlation of oceanic and atmospheric carbon reservoirs

Meaningful carbon–isotope stratigraphies for certain intervals of the Cretaceous have been produced where bulk organic matter has been characterized as dominantly terrestrial (Aptian [51,52], Cenomanian/Turonian boundary [53], Turonian–Maastrichtian [54]). These studies demonstrate that the carbon–isotope composition of bulk terrestrial organic-matter can be successfully used to show that the marine and terrestrial carbon cycles were coupled through geological time. However, there are inherent problems with the use of a bulk-rock method, in that (1) not every sample is characterized for percentage marine versus percentage terrestrial organic matter; (2) the terrestrial organic matter itself can be sourced from a variety of floral components with varying abundances between samples; and (3) the terrestrial organic matter may be composed of floral components from varying environments and thus varying isotopic signatures.

An alternative approach to using bulk terrestrial organic matter for carbon–isotope stratigraphy is to use discrete, identifiable floral components, such as charcoal, coalified fragments and leaf cuticle. Although a definitive, near-complete terrestrial $\delta^{13}C_{plant}$ record for the Valanginian has not been produced [55], other time periods within the Mesozoic have successfully been investigated, demonstrating the validity of the approach [48,52,55–62].

Gröcke et al. [58] and Hesselbo et al. [48,61] have demonstrated that terrestrial $\delta^{13}C_{plant}$ stratigraphies can be constructed from biostratigraphically well-constrained marine successions using recognizable plant fragments such as charcoal and coalified material. Such data are directly comparable with marine $\delta^{13}C$ stratigraphies and provide a basis with which to assign terrestrial sequences within a marine biostratigraphic framework, as shown by Robinson and Hesselbo [55] for the non-marine Wealden of southern England (mostly Hauterivian–Barremian).

1.4. Aim of the study

The potential for correlating marine and terrestrial sedimentary successions using $\delta^{13}C_{plant}$ records has been shown in numerous records for the Mesozoic. In this study we produced a fossil plant carbon–isotope stratigraphy for a shallow-marine Valanginian–Hauterivian succession from Kacha River, Crimea, Ukraine that is constrained by bio-(ammonite) and magneto-stratigraphy. The Valanginian period has been largely ignored in the study of Earth history, although more recently it has received attention [5,15,16,63,64]. The $\delta^{13}C_{plant}$ curve presented here allows us to evaluate whether the Upper Valanginian positive $\delta^{13}C$ excursion (previously recorded only in the marine record) is recorded in the atmospheric carbon reservoir.

2. Geological setting

The Early Cretaceous shallow-marine succession in the Crimean region of the Ukraine (Fig. 1) contains abundant fossil plant fragments preserved as charcoal and coal. The stratigraphic succession illustrated in Fig. 2 is a composite section measured from two localities. The lowermost, Valanginian-age part of the succession is located on the Kacha River, Rezanaya Mountain, on the outskirts of Verkhorechie Village (Section 23KP). The Hauterivian part is derived from the southern slope of Belaya Mountain on the northwestern outskirts of Verkhorechie Village (Section 28KP; Fig. 2). These Early Cretaceous sediments unconformably overlie folded metamorphic rocks that are Triassic–Middle Jurassic in age [65].

Fossil plant material was found throughout the Kacha River succession (with the exception of the upper part of the *Teschenites callidiscus* ammonite Zone). Other faunal components, including ammonites (see below), rare belemnites and bivalves, were also noted in the succession.

The lowermost part of the Valanginian succession is dominated by oolitic sands and silty sands: a log of this succession is shown in more detail in Ruffell et al. [66]. The Upper Valanginian–Lower Hauterivian is also dominated by clastic sedimentation, consisting of a series of bioturbated, inter-bedded shallow-marine silty sands and claystones. A stratigraphic gap (~5 m) is observed within the Upper Valanginian due to poor exposure.

2.1. Ammonite biostratigraphy

The ammonite biostratigraphic zonation of the Kacha River section (Fig. 2) has previously been defined [65,67–69]. The Berriasian to Lower Valanginian part of the succession including the *Thurmanni-*

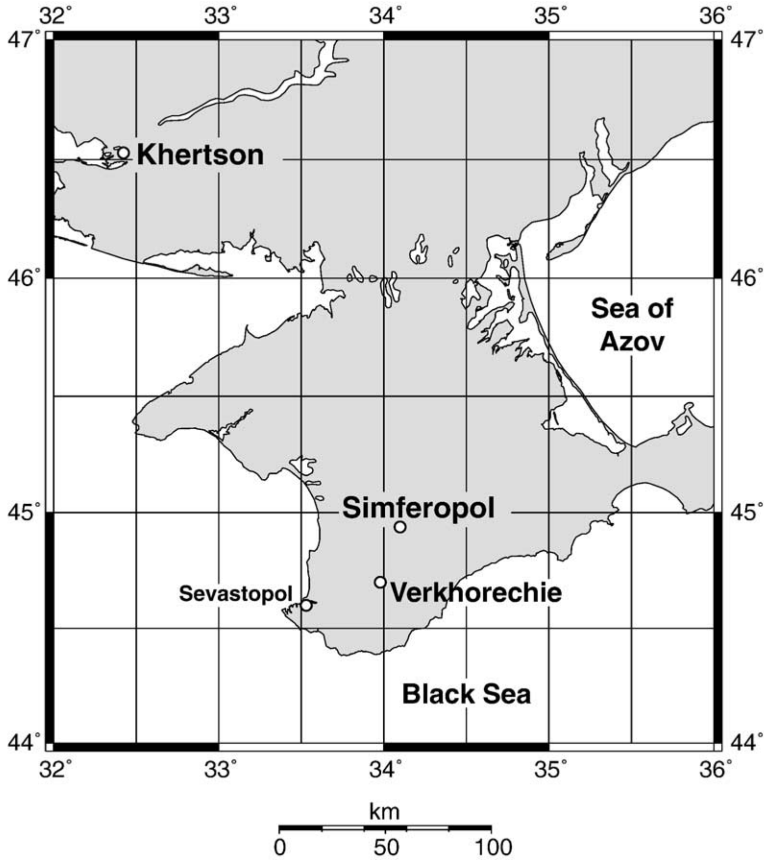

Fig. 1. GMT map of Crimea, Ukraine generated from the Online Map Creation website (http://www.aquarius.geomar.de/omc_intro.html). The stratigraphic sections investigated in this study are located alongside the Kacha River, near the village of Verkhorechie.

ceras otopeta–Thurmanniceras pertransiens ammonite Zones is relatively compact, with the *Busnardoites campylotoxus* ammonite Zone condensed to a single bed (Fig. 2). Following this is the *Neohoploceras submartini* ammonite Zone, which also contains the *Neocomites peregrinus* ammonite Subzone: no key species are found in this interval from the Kacha River (Fig. 2). The precise position of the *Himantoceras trinodosum* ammonite Zone is unclear as the definition of this zone is based upon a limited number of key ammonites. The Upper Valanginian is more expanded for the *T. callidiscus* and *Eleniceras tauricum* ammonite zones, although ammonite fossils become less common. The Valanginian/Hauterivian boundary as defined using ammonite biostratigraphy is at the base of the *Leopoldia desmoceroides* ammonite Zone at ~46.5 m above the base of Kacha River succession. Therefore, the ammonite stratigraphy generated from the Kacha River can be directly compared with that of the Tethyan scheme as outlined by Hoedemaeker et al. [70] and Reboulet and Atrops [71] (Fig. 3).

3. Methodology

Adhering sediment was removed from fossil plant samples through cleaning in deionized water in a sonification bath. Samples with cemented sediment were more vigorously cleaned with a brush. Samples were subsequently air-dried, and examined under a microscope to determine state of preservation: coal, charcoal and charcoal–coal (Plate I). Samples were divided if enough material was present for isotopic analysis: one half was archived, while the second half was ground to a fine powder in an agate mortar and pestle to form a homogenized sample. All samples were examined under a stereomicroscope while a representative group of samples were examined under an environmental scanning electron microscope. Use of the latter prevented the samples from being coated with gold, thus allowing subsequent geochemical analysis of that specific sample (if required).

All samples were treated with 3N HCl acid for a minimum of 1 h until all the carbonate had reacted. Carbon–isotope measurements were made on 95 sam-

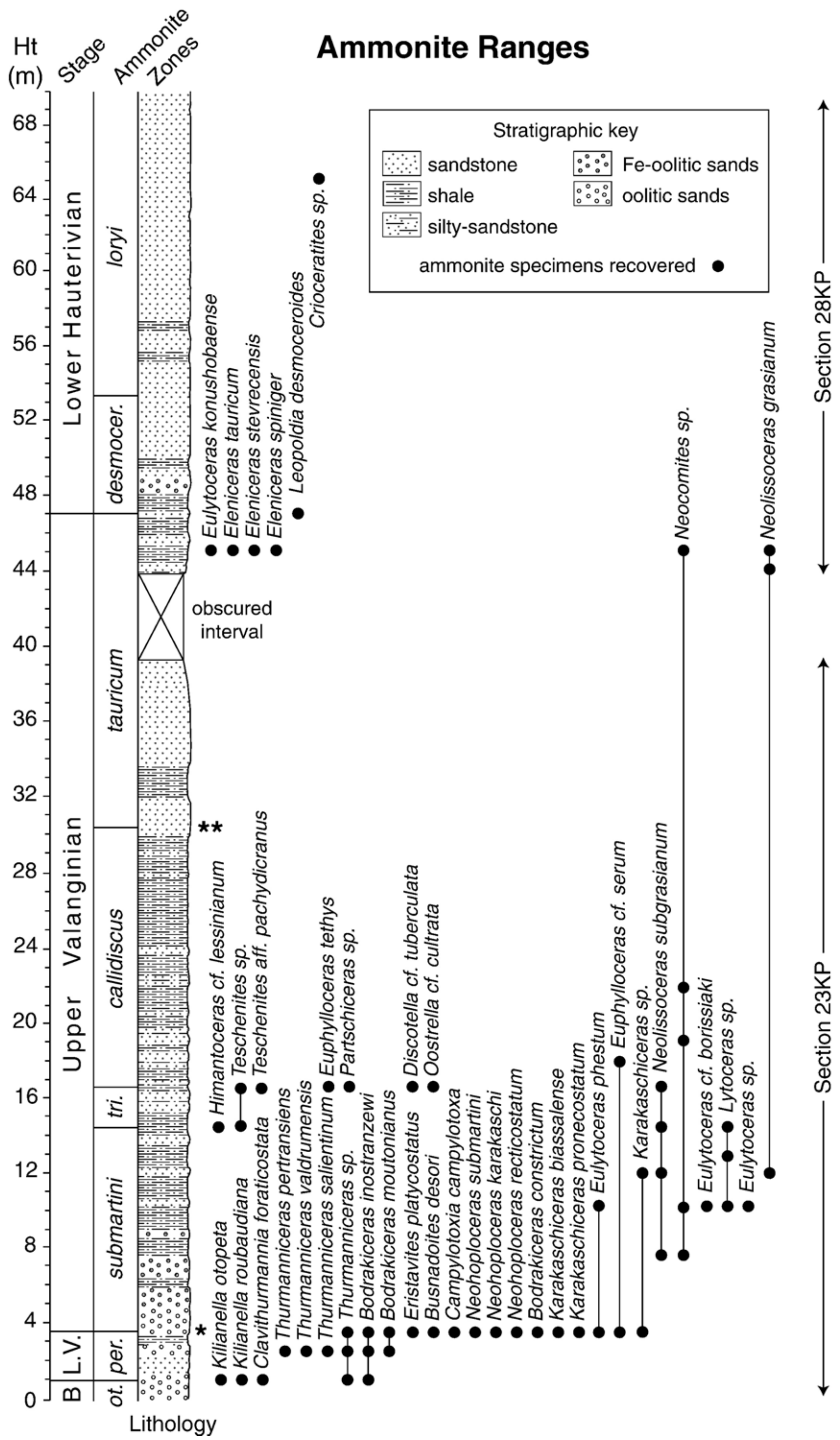

Fig. 2. The litho- and bio-stratigraphic succession at the Kacha River, Verkhorechie (a more detailed description of the sections investigated can be found in Baraboshkin [67]). The ammonite biostratigraphic zonation scheme is based on Baraboshkin and Yanin [65], Baraboshkin [67], Arkadiev et al. [68] and Baraboshkin and Mikhailova [69]. * = the *campylotoxa* ammonite Zone is condensed here to a single horizon; ** = the *callidiscus–tauricum* boundary has been assumed by Baraboshkin and Mikhailova [69] as mid-way between the last appearance of *Teschenites* sp. and first occurrence of *L. desmoceroides*. B = Berriasian. L.V. = Lower Valanginian. *ot*. = *otopeta*. *per*. = *pertransiens*. *tri*. = *trinodosum*. *desmocer*. = *desmoceroides*.

Stages		Tethyan Ammonite Zones and Subzones		Crimean Ammonite Zones and Subzones
Hauterivian	Upper	*P. ohmi*	*P. picteti*	*Psuedothurmannia catulloi*
			P. catulloi	
			P. ohmi	*Psuedothurmannia ohmi*
		Balerites balearis		*Milanowskia speetonensis*
		Plesiospitidiscus ligatus		*Speetoniceras inversum*
		Subsaynella sayni		*Crioceratitites duvali*
	Lower	*Lyticoceras nodosoplicatum*		*Lyticoceras nodosoplicatum*
		C. loryi	*O. (J.) jeannoti*	? *Crioceratites loryi*
			C. loryi	
		Acanthodiscus radiatus		*Leopoldia desmoceroides*
Valanginian	Upper	*C. furcillata*	*T. callidiscus*	*Eleniceras tauricum*
			C. furcillata	*Teschenites callidiscus*
		N. peregrinus	*O. (O.) nicklesi*	*Himantoceras trinodosum*
			N. peregrinus	
		Saynoceras verrucosum	*K. pronecostatum*	*Neohoploceras submartini*
			S. verrucosum	
	Lower	*Busnardoites campylotoxus*	*K. biassalense*	*Busnardoites campylotoxa*
			B. campylotoxus	
		Thurmanniceras pertransiens		*Thurmanniceras pertransiens*
B	U	*Thurmanniceras otopeta*		*Thurmanniceras otopeta*

Fig. 3. Biostratigraphic comparison between the Mediterranean [92] and Crimean [72] ammonite zonal schemes. B = Berriasian. U = upper. See ammonite Zone abbreviations in Fig. 2 caption.

ples of plant material from the Crimean succession (51 samples from Section 23KP, and 44 samples from Section 28KP) (Tables 1 and 2).

Powdered samples were weighed (between 1–3 mg), placed in tin capsules, and put in a rotating carousel for subsequent combustion in an elemental analyzer. The gas sample was subsequently purified and passed through a SIRA II Series 2 dual-inlet isotope-ratio mass-spectrometer for isotopic analysis. Carbon–isotope ratios were measured against an international standard (NBS-21) and expressed in the standard delta (δ) notation in per mil (‰) against the internationally accepted standard notation, Vienna Peedee Belemnite (VPDB). Analytical reproducibility of replicate samples using this method was better than ± 0.1‰.

4. Results

The isotope data are shown in Tables 1 and 2, and graphically in Fig. 4. The carbon–isotope results are divided into two main groups (Valanginian = Section 23KP; middle Hauterivian = Section 28KP) based on the two stratigraphic sections investigated. $\delta^{13}C_{plant}$ average and standard deviations of the population for Section 23KP and Section 28KP are -20.94‰ (± 1.30‰) and -22.46‰ (± 0.83‰), respectively. The most positive $\delta^{13}C_{plant}$ value is from sample 23KP-7 (-18.17‰), while the most negative is from sample 23KP-50 (-24.05‰). Percentage carbon (%C) is generally low compared with modern charcoalified plant remains (Tables 1 and 2), which ranges

Plate I. Scanning electron microscope images showing the different states of preservation found in fossil plant fragments from Kacha River, Verkhorechie, Crimea. All scale bars represent 100 μm. (A) 23KP-1 — charcoal. (B) 23KP-1 — charcoal (close-up of A). Note, the very fine sediment infilling the plant cells, with the occasional large sand grains (arrows). (C) 23KP-45 — charcoal–coal. On the surface this fragment looks like coal, but note the broken surface in the top left hand corner (arrow). (D) 23KP-45 — charcoal–coal (close-up of C). Plant cells are still visible (arrows), although through the process of compression, combined with heating has led to cell homogenization. (E) 28KP-40 — coal. The blocky nature of this fragment led us to identify it as coal, but on closer inspection linear plant cell structure is still preserved (arrows), thus suggesting that high-magnification identification may be a more suitable identifying process for future studies. (F) 23KP-42 — charcoal–coal. Note, the secondary calcite infillings of the plant cells, highlighting the requirement that all terrestrial fragments must be 'decarbonated' prior to isotopic analysis.

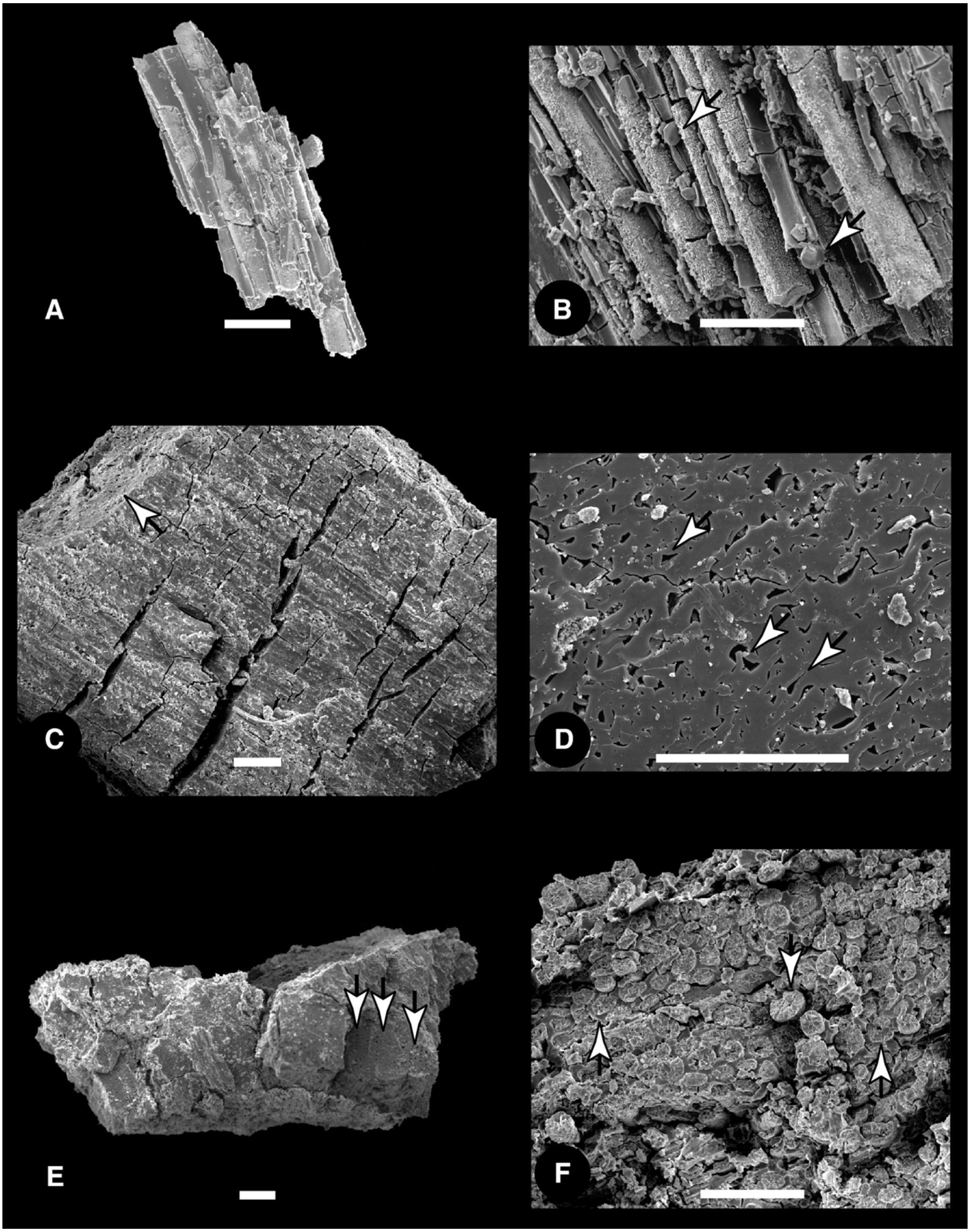

A
B
C
D
E
F

Table 1
δ^{13}C data of fossil plant fragments from Kacha River, Rezanaya Mountain, Verkhorechie Village (23KP Section)

Sample ID	Height (m)	$\delta^{13}C_{plant}$ (‰)	%C	Preservation
23KP-48	1.20	−23.35	47.71	Coal
23KP-50	2.90	−24.05	20.21	Charcoal
23KP-52	3.60	−23.74	37.99	Coal
23KP-51	3.65	−22.37	33.78	Ch–coal
23KP-45	6.40	−23.71	25.53	Ch–coal
23KP-47	6.60	−22.61	48.77	Ch–coal
23KP-40	7.30	−22.95	41.98	Coal
23KP-46	10.00	−23.83	23.94	Charcoal
23KP-42	11.20	−20.94	29.11	Ch–coal
23KP-44	11.60	−21.30	28.93	Charcoal
23KP-43	12.70	−20.41	39.95	Charcoal
23KP-26	13.40	−22.40	29.92	Charcoal
23KP-24	13.80	−20.11	33.64	Ch–coal
23KP-25	13.80	−20.52	44.06	Ch–coal
23KP-23	13.90	−21.26	36.86	Charcoal
23KP-21	14.70	−20.58	50.83	Coal
23KP-22	14.70	−21.04	36.83	Charcoal
23KP-19	14.95	−21.78	26.63	Charcoal
23KP-20	14.95	−21.22	46.48	Coal
23KP-18	15.00	−19.47	45.05	Coal
23KP-49	15.30	−20.95	42.99	Ch–coal
23KP-17	15.65	−19.91	26.71	Charcoal
23KP-33	16.05	−18.89	30.96	Charcoal
23KP-29	16.10	−20.28	35.45	Ch–coal
23KP-32	16.25	−19.79	37.98	Coal
23KP-27	16.50	−20.13	24.13	Charcoal
23KP-28	16.55	−20.94	40.82	Charcoal
23KP-30	16.75	−20.23	42.95	Ch–coal
23KP-31	16.80	−19.47	37.85	Ch–coal
23KP-34	17.30	−19.38	42.73	Charcoal
23KP-6	18.00	−21.22	40.93	Ch–coal
23KP-8	18.00	−19.78	26.63	Charcoal
23KP-7	18.25	−18.17	31.69	Charcoal
23KP-2	18.60	−20.20	45.51	Charcoal
23KP-1	18.65	−19.75	30.39	Charcoal
23KP-4	18.70	−20.64	45.11	Charcoal
23KP-3	18.80	−21.21	50.47	Coal
23KP-9	18.80	−20.90	25.14	Charcoal
23KP-5	19.15	−20.70	28.55	Charcoal
23KP-10	20.00	−21.08	47.48	Coal
23KP-11	20.20	−20.73	51.05	Charcoal
23KP-12	20.80	−21.90	34.84	Coal
23KP-16	21.20	−21.08	47.48	Ch–coal
23KP-13	21.50	−19.49	37.29	Charcoal
23KP-14	21.70	−20.42	49.56	Ch–coal
23KP-15	22.10	−20.19	44.37	Charcoal
23KP-38	22.80	−20.76	34.20	Charcoal
23KP-39	26.40	−19.37	38.64	Ch–coal
23KP-37	28.80	−20.50	40.99	Charcoal
23KP-36	29.30	−20.30	35.69	Ch–coal
23KP-35	34.00	−21.72	47.13	Charcoal

Preservation: coal, charcoal and charcoal–coal (Ch–coal). %C derived from combustion during isotopic analysis.

Table 2
δ^{13}C data of fossil plant fragments from Belaya Mountain, north–western outskirts of Verkhorechie Village (28KP Section)

Sample ID	Height (m)	$\delta^{13}C_{plant}$ (‰)	%C	Preservation
28KP-2	44.00	−21.86	34.51	Ch–coal
28KP-3	44.00	−22.23	38.41	Ch–coal
28KP-1	44.10	−21.93	50.07	Charcoal
28KP-6	44.20	−23.79	23.77	Charcoal
28KP-7	44.20	−23.93	36.16	Coal
28KP-4	45.10	−22.61	42.57	Ch–coal
28KP-8	45.75	−23.17	39.28	Charcoal
28KP-5	46.00	−21.66	39.49	Coal
28KP-12	46.80	−22.94	38.63	Coal
28KP-11	47.00	−22.62	23.73	Ch–coal
28KP-10	47.05	−22.62	39.10	Charcoal
28KP-9	47.15	−22.38	45.39	Charcoal
28KP-14	48.50	−21.58	37.25	Ch–coal
28KP-15	48.50	−21.14	52.01	Charcoal
28KP-16	48.65	−22.37	34.93	Ch–coal
28KP-13	49.50	−23.45	43.89	Charcoal
28KP-21	50.50	−22.36	26.02	Charcoal
28KP-19	50.80	−21.21	48.18	Charcoal
28KP-20	50.80	−21.79	27.90	Charcoal
28KP-16	50.90	−22.49	30.76	Ch–coal
28KP-17	51.05	−21.88	39.58	Charcoal
28KP-18	51.15	−21.09	37.03	Charcoal
28KP-22	51.60	−23.59	55.98	Ch–coal
28KP-23	52.40	−24.04	41.82	Charcoal
28KP-24	52.40	−22.51	23.33	Charcoal
28KP-25	52.65	−22.78	36.79	Charcoal
28KP-26	53.80	−22.84	31.73	Charcoal
28KP-31	54.80	−22.43	20.71	Coal
28KP-28	54.85	−22.14	30.81	Ch–coal
28KP-30	54.85	−23.78	47.24	Charcoal
28KP-29	54.90	−23.59	36.23	Ch–coal
28KP-32	55.40	−21.05	33.43	Charcoal
28KP-39	56.20	−21.21	29.03	Charcoal
28KP-40	56.50	−21.08	26.42	Coal
28KP-27	57.30	−22.36	38.41	Ch–coal
28KP-41	57.60	−23.05	23.76	Ch–coal
28KP-38	58.30	−22.77	20.26	Charcoal
28KP-42	58.30	−23.85	37.62	Charcoal
28KP-37	58.90	−21.74	35.71	Charcoal
28KP-34	59.80	−22.21	31.98	Brown-ch
28KP-35	60.00	−21.78	33.45	Charcoal
28KP-43	61.40	−22.49	40.76	Ch–coal
28KP-36	62.30	−22.53	34.86	Coal
28KP-33	63.00	−23.21	31.36	Charcoal

Brown-ch represents a sample that was brown in colour, but preserved like charcoal. See Table 1 for additional information.

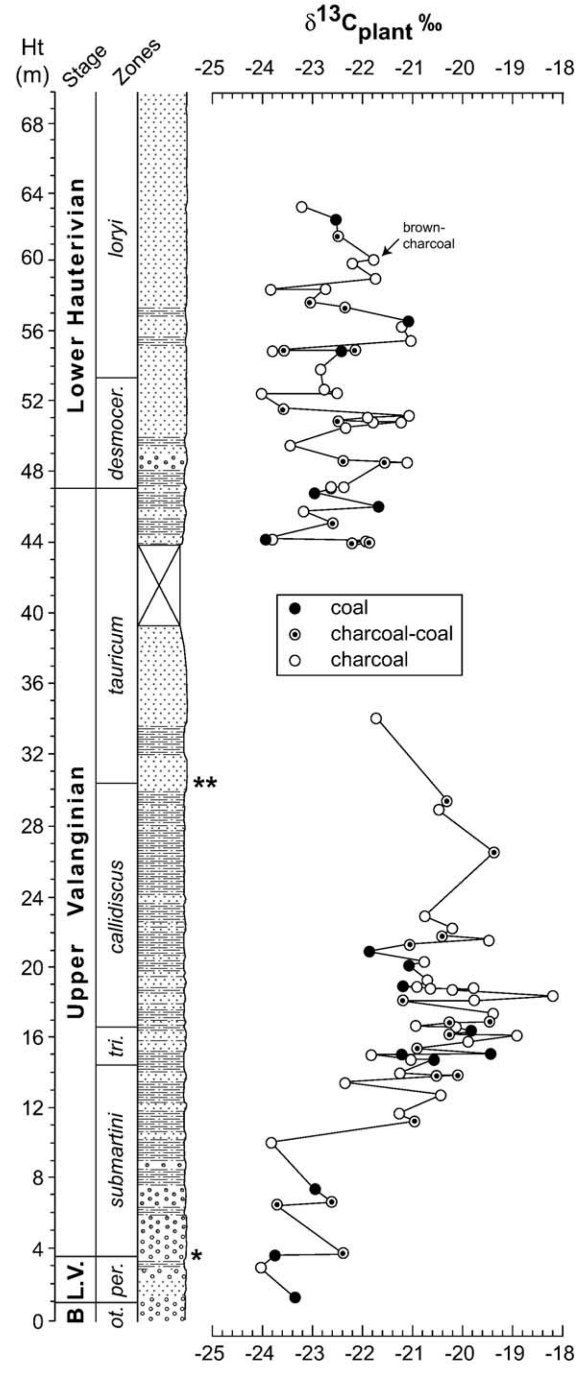

Fig. 4. $\delta^{13}C_{plant}$ data from the Valanginian–Hauterivian at Kacha River, Verkhorechie. See Fig. 2 for additional information. Note the brown charcoal sample.

between 45% and 80% depending on the temperature of the fire [Gröcke, unpub. data]: this may be caused by the infilling of plant cells with sediment, and thus sample weights being greater than a modern sample of charcoal. Although %C is low, the average for each stratigraphic section is very similar (Section 23KP = 37.72% ± 8.25%; Section 28KP = 35.69% ± 8.22%), suggesting that there is no major difference in the degree of any potential diagenetic alteration at each section, and that the observed trends in $\delta^{13}C_{plant}$ are not related to %C. Although the plant material preserved ranged from charcoal to coal, this made no difference in the overall long-term trend of the $\delta^{13}C_{plant}$ curve. This has previously been documented for Toarcian and Aalenian–Bajocian successions in the Jurassic [48,61].

$\delta^{13}C_{plant}$ values fluctuate between −22‰ and −24‰ during the *pertransiens–verrucosum* ammonite Zones, but rise rapidly in the upper *verrucosum* Zone to values around −22‰ to −20‰. During the *trinodosum* and *callidiscus* ammonite Zones $\delta^{13}C_{plant}$ values remain more positive (between −21‰ and −19‰) with the most positive value occurring in the lower *callidiscus* Zone (−18‰). In the upper *callidiscus* Zone $\delta^{13}C_{plant}$ values show a trend towards pre-excursion values, although sample density becomes less in this part of the stratigraphic section and this is also where the ~5 m stratigraphic gap is located. $\delta^{13}C_{plant}$ values in the *leopoldina* and *loryi* ammonite Zones (Hauterivian) remain relatively constant at ~−22.5‰, with some internal fluctuation (between −24‰ and −21‰). The amount of scatter in the Kacha River data is similar to that noted in previous comparable studies [55,58].

5. Discussion

5.1. Correlating the ocean–atmosphere carbon reservoirs

The Valanginian–Hauterivian $\delta^{13}C_{plant}$ curve from Kacha River, Verkhorechie Village, Crimea records the positive $\delta^{13}C$ excursion (Fig. 5) that was previously known only from marine carbonate and marine organic matter [1,38,50]. The lower part of the Kacha River succession, although condensed, has relatively good ammonite biostratigraphic control and the resultant $\delta^{13}C_{plant}$ curve corresponds well with the Tethyan marine $\delta^{13}C_{carb}$ curve (Fig. 5). Initiation of the positive $\delta^{13}C_{plant}$ excursion occurs in the Crimean *submartini* ammonite Zone which, based on the correlations of Baraboshkin et al. [72], would equate to the *verrucosum* Mediterranean ammonite zone.

The initiation of this positive $\delta^{13}C$ excursion within Tethyan marine carbonates occurs at the *campylotoxus–verrucosum* zonal boundary [34,73], although Henning et al. [38] observed that the initiation of the Upper Valanginian carbon–isotope excursion occurred wholly

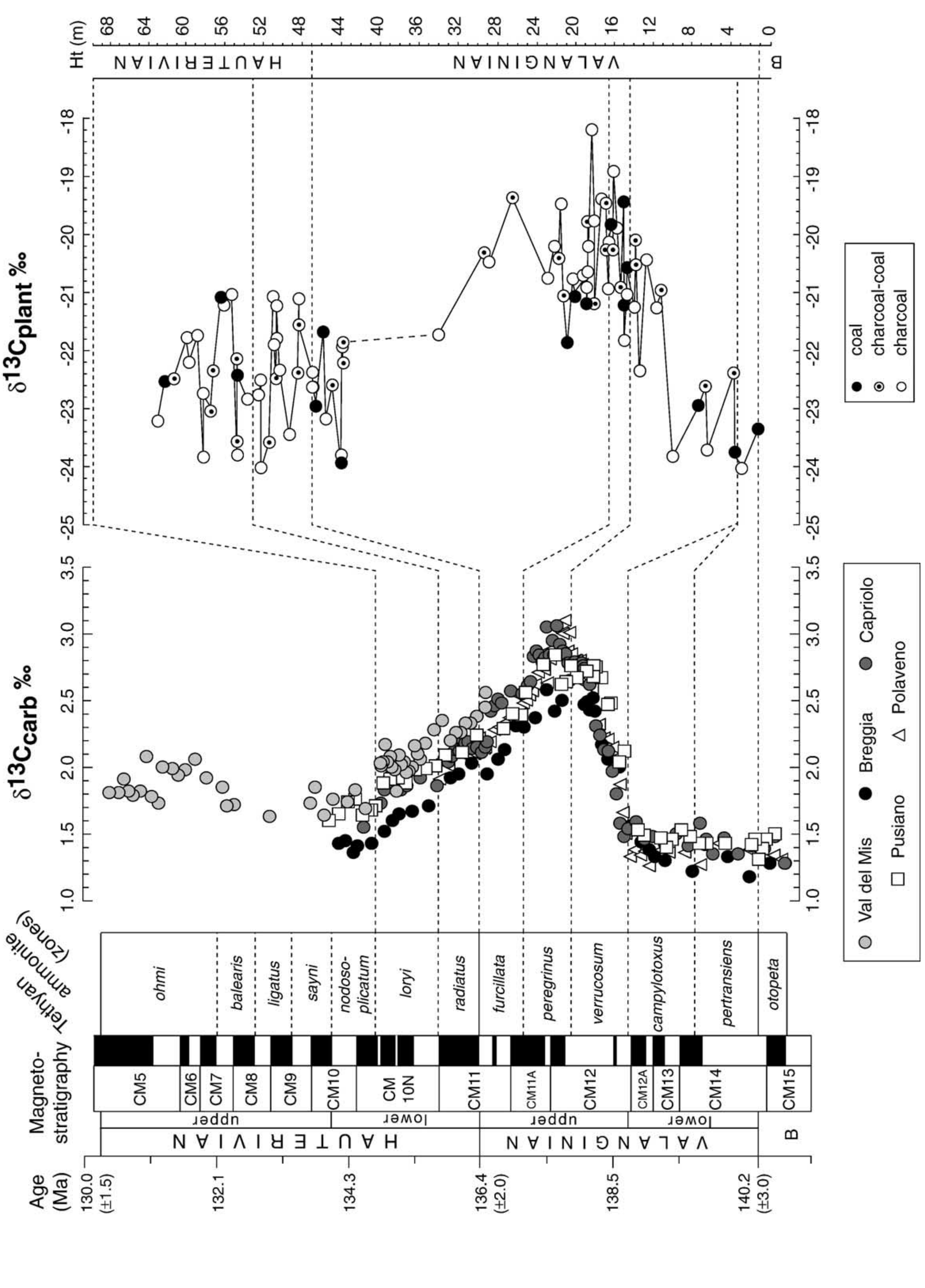

δ13Cplant ‰
δ13Ccarb ‰
Ht (m)
Age (Ma)
Magneto-stratigraphy
Tethyan ammonite (zones)
HAUTERIVIAN
VALANGINIAN
B
upper
lower
coal
charcoal-coal
charcoal
Val del Mis
Breggia
Capriolo
Pusiano
Polaveno
ohmi
balearis
ligatus
sayni
nodoso-plicatum
loryi
radiatus
furcillata
peregrinus
verrucosum
campylotoxus
pertransiens
otopeta
CM5
CM6
CM7
CM8
CM9
CM10
CM 10N
CM11
CM11A
CM12
CM12A
CM13
CM14
CM15

within the *campylotoxus* ammonite Zone. Channell et al. [36,74] placed the initiation of the positive $\delta^{13}C$ excursion within the *Calcicalathina oblongata* nannofossil Zone. The biostratigraphy of these Italian sections is based largely on nannoplankton data [1,36,74], as they are poorly characterized by ammonite biostratigraphy, especially across the Valanginian–Hauterivian transition. The ammonite scale used is based on a correlation of nannoplankton and ammonite distributions in France, Spain and Germany in particular, where ammonites are much more common. Channell et al. [74] correlate the *verrucosum* ammonite Zone with the interval between the CM11A and CM12 magnetochron Zones. It is at the top of magnetochron Zone CM12 that Weissert and Erba [34] place the onset of the Valanginian $\delta^{13}C$ excursion. Gradstein et al. [5] place the *verrucosum* ammonite Zone at the base of magnetochron Zone CM12. Recent paleomagnetic data obtained from the Valanginian–Hauterivian succession at Verkhorechie Village, Kacha River [75] suggest that the peak of the $\delta^{13}C_{plant}$ positive excursion occurs at the top of magnetochron Zone CM12, thus confirming earlier studies [34,38,74].

The peak of the positive $\delta^{13}C_{plant}$ curve corresponds well biostratigraphically between Crimea (within the *trinodosum–callidiscus* ammonite Zones) and the Mediterranean (within the *trinodosum* ammonite Zone) [17,34,73]. For the upper part of the Verkhorechie Village section the ammonite and magnetochron constraint becomes less robust with poor ammonite recovery and little change in the magneto-stratigraphy, respectively. Nevertheless, the $\delta^{13}C_{plant}$ data does not contradict a Lower Hauterivian age assignment, although the gradual decline to pre-excursion values in the Upper Valanginian is not recorded due to poor sample recovery (Fig. 4). In addition, the relatively high degree of scatter in $\delta^{13}C_{plant}$ from the Lower Hauterivian disguises the gradual decline in carbon–isotope ratios as seen in the Tethyan carbonate record (Fig. 5).

Previous studies of long-term $\delta^{13}C_{plant}$ records in the Mesozoic have shown that the timing and duration of carbon–isotope excursions are synchronous in marine carbonate, marine organic matter and terrestrial organic matter [48,51–53,58]. Any discrepancy in the correlation between Crimean and Italian $\delta^{13}C$ curves in terms of biostratigraphy is likely due to problems associated with ammonite and nannofossil correlations. Nonetheless, within the limits of biostratigraphic resolution, there appears to be no time lag between carbon–isotope excursions (both the initiation and decay) recorded by both oceanic and atmospheric proxies for the Valanginian–Hauterivian transition (Fig. 5).

Table 3
$\Delta\delta$ relations across the Upper Valanginian positive $\delta^{13}C$ excursion

Valanginian $\delta^{13}C$ excursion					
$\Delta\delta$	Locality	Pre	Peak	Post	Source
$\delta^{13}C_{carb}$–$\delta^{13}C_{org}$	DSDP Site 535	29.9	29.4	29.1	[91]
$\delta^{13}C_{carb}$–$\delta^{13}C_{org}$	Polaveno	27.8	28.1		[1]
$\delta^{13}C_{carb}$–$\delta^{13}C_{org}$	Rio Corna	28.2	27.0		[1]
$\delta^{13}C_{carb}$–$\delta^{13}C_{plant}$	Crimea	24.6	22.4	24.2	Fig. 5, this study

5.2. *pCO_2 fluctuations and a $\Delta\delta^{13}C_{carb–plant}$ reconstruction*

Delta–delta ($\Delta\delta = \delta^{13}C_{carb}$–$\delta^{13}C_{org}$) relationships have been applied in paleoceanographic carbon–isotope investigations in order to discern fluctuations in carbon–isotope fractionation in organic matter, and thus used as a proxy for pCO_2 concentrations [37,47,76]. Since plants may also be considered in the same manner [54,56–58,77,78], we have calculated the $\Delta\delta$ dataset between our terrestrial $\delta^{13}C_{plant}$ record (Fig. 4) and the composite $\delta^{13}C_{carb}$ record from the Tethyan region (Fig. 5). Table 3 shows a summary of the $\delta^{13}C$ records of organic matter through the Valanginian period. It is evident from the few records available for the Valanginian that there is a lack of a $\Delta\delta$ shift in the marine records prior to and at the peak of the $\delta^{13}C$ excursion, whereas there is a distinct +2‰ shift between the marine carbonate and terrestrial plant record from Crimea. Although more detailed marine and terrestrial records are required to determine if this $\Delta\delta$ shift is in fact significant, it suggests a very intriguing paleoenvironmental event.

Modern $\delta^{13}C_{plant}$ studies tend to indicate a change in pCO_2 causes a shift in photosynthetic isotope frac-

Fig. 5. Valanginian–Hauterivian $\delta^{13}C$ correlation between the composite Tethyan bulk $\delta^{13}C_{carb}$ curve and the $\delta^{13}C_{plant}$ curve from Kacha River, Crimea. The Tethyan bulk carbonate $\delta^{13}C$ curve is based upon data from Lini et al. [1] and Channell et al. [36]. Tethyan $\delta^{13}C$ data are from Breggia, Capriolo, Polaveno, Pusiano and Val del Mis [1,36]. Timescale is from Gradstein et al. [5]. An age-model was constructed for each section by assigning ages to polarity chron boundaries, and thus points in the rock record. By assuming a constant sedimentation rate during each polarity chron it was possible to assign an age to each isotopic data point. In order to achieve this, magneto-stratigraphic and biostratigraphic zonations have been adopted directly from Channell and Erba [3] and Channell et al. [74,93,94], and the latest ammonite zonation revision presented by Hoedemaeker et al. [92]. $\delta^{13}C$ correlations are based on bio- (ammonite) and magneto-stratigraphic data from the Kacha River succession. Note, the Crimea $\delta^{13}C_{plant}$ data is plotted versus height and not an age-model as the Tethyan $\delta^{13}C_{carb}$ data.

tionation and that a 10% decrease in pCO_2 leads to a +0.5‰ change in $\delta^{13}C_{plant}$ [57,79,80]. Therefore, the +2‰ change in $\Delta\delta_{carb-plant}$ from the pre-peak to peak segment of the Upper Valanginian $\delta^{13}C$ positive excursion would indicate a drop in atmospheric pCO_2 in the order of ~40%. Some contribution to this +2‰ shift in $\Delta\delta_{carb-plant}$ may be caused by other paleoenvironmental factors such as an increase in temperature and/or salinity affecting the $\delta^{13}C$ values of plants from the Kacha River region. What is difficult to explain is the lack of a similar shift in $\Delta\delta_{carb-org}$ in the oceanic records, although the drop of ~1.2‰ from Rio Corna would also indicate a drop in pCO_2. Erba and Tremolada [64] recently proposed an oceanic anoxic event during the Upper Valanginian and it has been suggested that periods of global organic carbon burial are associated with a concomitant drawdown of CO_2 [81,82].

Since the $\delta^{13}C$ of the dissolved bicarbonate–carbonate reservoir is determined primarily through the partitioning of sedimentary carbon into the organic and inorganic reservoirs, an organic carbon burial event, such as an oceanic anoxic event, would result in a positive $\delta^{13}C$ excursion in the ocean–atmosphere system. Such an event would lead to a drawdown of pCO_2 and an absolute increase in atmospheric oxygen. A similar mechanism has been proposed by Jahren et al. [62] to account for the terrestrial $\delta^{13}C_{plant}$ record of the Aptian OAE.

5.3. A Late Valanginian icehouse?

Erba et al. [63] recently proposed that the Valanginian event is equivalent to an oceanic anoxic event based on the $\delta^{13}C_{carb}$ record. However, at present it does not appear that there was a discrete interval of time in the Upper Valanginian during which global organic–carbon burial rates were significantly elevated; the major criterion for defining an oceanic anoxic event [82]. Notwithstanding this, present evidence suggests a cooling episode during the Lower to Upper Valanginian [22,23,28,34,83–85], which based on our understanding of the Earth climate system would also indicate a decrease in pCO_2. Recently, Dessert et al. [86] indicated that the weathering of basalts (i.e., the Paranà-Etendeka continental flood basalts) may induce a drop in pCO_2, which would be consistent with a cooling episode.

Our data and analysis support the recent suggestions of Erba et al. [63]: the Late Valanginian experienced the eruption of the Paranà-Etendeka continental flood basalts, an increase in surface-water fertility and production, the development of localized black shales, boreal excursions of marine fauna and increases in global continental weathering. However, Erba et al. [63] suggest that the cooling event post-dated the initiation of the Valanginian $\delta^{13}C$ positive event based on marine microfossils. Table 3 indicates that the oceanic realm did record a significant pCO_2 change over the Valanginian event, and thus a shift in microfossil assemblages may be induced by paleotemperature and/or seawater chemistry changes rather than dissolved oceanic pCO_2. The $\delta^{13}C_{plant}$ data suggests that the atmospheric realm experienced pCO_2 decreases concurrent with the peak of the Valanginian event. pCO_2 levels in the atmosphere are also affected by other factors, such as silicate weathering, the net global depositional rate of calcium carbonate, and volcanism [39,42,87,88].

We suggest that the Upper Valanginian was in fact a period that endured a short-lived (<3 Myr) cooling event and does not (as previously suggested) appear to represent the initiation of the Cretaceous greenhouse period [1]. The possibility that the paleoenvironment prior to and/or after the Upper Valanginian $\delta^{13}C$ positive event was experiencing greenhouse conditions is not implausible. A closer examination of other positive $\delta^{13}C$ events in geologic time may in fact reveal themselves to represent periods of global cooling. It is becoming increasingly apparent that the notion of an equable, greenhouse climate throughout the Cretaceous is erroneous. Geological warm periods were occasionally interrupted by episodes of cooling and/or glaciation, either locally or globally, and these short-lived episodes are linked with pCO_2 changes in the ocean–atmosphere system [14,17,24,32,89,90].

Acknowledgements

This project was funded through a Natural Sciences and Engineering Research Council Discovery Grant (DRG) and a Royal Society Research Grant (GP and AR). Our thanks also extend to Andre Guzikov (Saratov) for assistance in the field. Fossil coal and charcoal SEM images were taken at the Scanning Electron Microscope Unit, University of Plymouth. Elisabetta Erba and Bas van de Schootbrugge are thanked for excellent reviews that greatly improved and focused this manuscript.

References

[1] A. Lini, H. Weissert, E. Erba, The Valanginian carbon isotope event: a first episode of greenhouse climate conditions during the Cretaceous, Terra Nova 4 (1992) 374–384.

[2] K.B. Föllmi, H. Weissert, M. Bisping, H. Funk, Phosphogenesis, carbon–isotope stratigraphy, and carbonate-platform evolution

along the Lower Cretaceous northern Tethyan margin, Geol. Soc. Amer. Bull. 106 (1994) 729–746.
[3] J.E.T. Channell, E. Erba, Early Cretaceous polarity chrons CM0 and CM11 recorded in northern Italian land sections near Brescia, Earth Planet. Sci. Lett. 108 (1995) 161–179.
[4] V. Courtillot, C. Jaupart, I. Manighetti, P. Tapponnier, J. Besse, On causal links between flood basalts and continental breakup, Earth Planet. Sci. Lett. 166 (1999) 177–195.
[5] F. Gradstein, J. Ogg, A. Smith, A Geologic Time Scale, Cambridge University Press, Cambridge, 2004.
[6] K. Wallmann, Controls on the Cretaceous and Cenozoic evolution of seawater composition, atmospheric CO_2 and climate, Geochim. Cosmochim. Acta 65 (2001) 3005–3025.
[7] K.W. Hansen, K. Wallmann, Cretaceous and Cenozoic evolution of seawater composition, atmospheric O_2 and CO_2: a model perspective, Am. J. Sci. 303 (2003) 94–148.
[8] E. Tajika, Carbon cycle and climate change during the Cretaceous inferred from a biogeochemical carbon cycle model, Isl. Arc 8 (1999) 293–303.
[9] S.A. Robinson, J.E. Andrews, S.P. Hesselbo, J.D. Radley, P.F. Dennis, I.C. Harding, P. Allen, Atmospheric $p\mathrm{CO}_2$ and depositional environment from stable-isotope geochemistry of calcrete nodules (Barremian, Lower Cretaceous, Wealden Beds, England), J. Geol. Soc. (Lond.) 159 (2002) 215–224.
[10] C.E. Jones, H.C. Jenkyns, A.L. Coe, S.P. Hesselbo, Strontium isotopic variations in Jurassic and Cretaceous seawater, Geochim. Cosmochim. Acta 58 (1994) 3061–3074.
[11] O.G. Podlaha, J. Mutterlose, J. Veizer, Preservation of δ^{18}O and δ^{13}C in belemnite rostra from the Jurassic/Early Cretaceous successions, Am. J. Sci. 298 (1998) 324–347.
[12] D.R. Gröcke, Isotope Stratigraphy and Ocean-Atmosphere Interactions in the Jurassic and Early Cretaceous. D.Phil. Thesis, University of Oxford, 2001, 78 pp.
[13] G.D. Price, D.R. Gröcke, Strontium–isotope stratigraphy and oxygen and carbon-isotope variation during the Middle Jurassic–Early Cretaceous of the Falkland Plateau, South Atlantic, Palaeogeogr. Palaeoclimatol. Palaeoecol. 183 (2002) 209–222.
[14] D.R. Gröcke, G.D. Price, A.H. Ruffell, J. Mutterlose, E. Baraboshkin, Isotopic evidence for Late Jurassic–Early Cretaceous climate change, Palaeogeogr. Palaeoclimatol. Palaeoecol. 202 (2003) 97–118.
[15] J.M. McArthur, J. Mutterlose, G.D. Price, P.F. Rawson, A. Ruffell, M.F. Thirlwall, Belemnites of Valanginian, Hauterivian and Barremian age: Sr-isotope stratigraphy, composition (^{87}Sr/^{86}Sr, δ^{13}C, δ^{18}O, Na, Sr, Mg), and palaeo-oceanography, Palaeogeogr. Palaeoclimatol. Palaeoecol. 202 (2004) 253–272.
[16] G.D. Price, A.H. Ruffell, C.E. Jones, R.M. Kalin, J. Mutterlose, Isotopic evidence for temperature variation during the Early Cretaceous (Late Ryazanian–mid Hauterivian), J. Geol. Soc. (Lond.) 157 (2000) 335–343.
[17] B. van de Shootbrugge, K.B. Föllmi, L.G. Bulot, S.J. Burns, Paleoceanographic changes during the Early Cretaceous (Valanginian–Hauterivian): evidence from oxygen and carbon stable isotopes, Earth Planet. Sci. Lett. 181 (2000) 15–31.
[18] F.H. Dorman, E.D. Gill, Oxygen isotope palaeotemperature measurements on Australian fossils, Proc. R. Soc. Vic. 71 (1959) 73–98.
[19] J.L. DeLurio, L.A. Frakes, Glendonites as a paleoenvironmental tool: implications for Early Cretaceous high latitude climates in Australia, Geochim. Cosmochim. Acta 63 (1999) 1034–1048.
[20] P.W. Ditchfield, High northern palaeolatitude Jurassic–Cretaceous palaeotemperature variation: new data from Kong Karls Land, Svalbard, Palaeogeogr. Palaeoclimatol. Palaeoecol. 130 (1997) 163–175.
[21] J. Mutterlose, K. Kessels, Early Cretaceous nannofossil variation from the Norwegian North Sea and Antarctic Shelf reflect latitudinal climate belts, Palaeogeogr. Palaeoclimatol. Palaeoecol. 156 (2000) 173–187.
[22] J. Mutterlose, H. Brumsack, S. Flögel, W. Hay, C. Klein, U. Langrock, M. Lipinski, W. Ricken, E. Söding, R. Stein, O. Swientek, The Greenland–Norwegian Seaway: a key area for understanding Late Jurassic to Early Cretaceous paleoenvironments, Paleoceanography 18 (2003), doi:10.1029/2001PA000625.
[23] E. Kemper, Das Klima der Kreide-Zeit, Geol. Jahrb. A96 (1987) 5–185.
[24] L.A. Frakes, J.E. Francis, A guide to Phanerozoic cold polar climates from high latitude ice-rafting in the Cretaceous, Nature 333 (1988) 547–549.
[25] G.D. Price, The evidence and implications of polar ice during the Mesozoic, Earth Sci. Rev. 48 (1999) 183–210.
[26] E. Kemper, Über Kalt und Warmzeiten der Unterkreide, Zitteliana 10 (1983) 359–369.
[27] M.E. Kaplan, Calcite pseudomorphoses in Jurassic and Lower Cretaceous deposits of the Northern Area of Eastern Siberia, Geol. Geofiz. 19 (1978) 62–70.
[28] J.A. Tarduno, R.D. Cottrell, P. Lippert, M. Friedman, Extreme climates recorded in the Cretaceous High Arctic, JOI/USSAC Workshop on Cretaceous Climate and Ocean Dynamics, Florissant, Colorado, Abstract Volume, 2002, p. 76.
[29] N.F. Alley, L.A. Frakes, First known Cretaceous glaciation: Livingston Tillite Member of the Cadna-owie Formation, South Australia, Aust. J. Earth Sci. 50 (2003) 139–144.
[30] A. Dalland, Erratic clasts in the Lower tertiary deposits of Svalbard-evidence of transport by winter ice, Norsk Polarin. Arbok. 1976 (1977) 151–165.
[31] O.G. Epshteyn, Mesozoic–Cenozoic climates of northern Asia and glacial-marine deposits, Int. Geol. Rev. 20 (1978) 49–58.
[32] H.M. Stoll, D.P. Schrag, Evidence for glacial control of rapid sea level changes in the Early Cretaceous, Science 272 (1996) 1771–1774.
[33] T.D. Frank, M.A. Arthur, W.E. Dean, Diagenesis of Lower Cretaceous pelagic carbonates, North Atlantic: paleoceanographic signals obscured, J. Foraminiferal Res. 29 (1999) 340–351.
[34] H. Weissert, E. Erba, Volcanism, CO_2 and palaeoclimate: a Late Jurassic–Early Cretaceous carbon and oxygen isotope record, J. Geol. Soc. London 161 (2004) 695–702.
[35] H. Weissert, C-isotope stratigraphy, a monitor of paleoenvironmental change: a case study from the Early Cretaceous, Surv. Geophys. 10 (1989) 1–61.
[36] J.E.T. Channell, E. Erba, A. Lini, Magnetostratigraphic calibation of the Late Valanginian carbon isotope event in pelagic limestones from Northern Italy and Switzerland, Earth Planet. Sci. Lett. 118 (1993) 145–166.
[37] H. Weissert, A. Lini, K.B. Föllmi, O. Kuhn, Correlation of Early Cretaceous carbon isotope stratigraphy and platform drowning events: a possible link? Palaeogeogr. Palaeoclimatol. Palaeoecol. 137 (1998) 189–203.
[38] S. Henning, H. Weissert, L. Bulot, C-isotope stratigraphy, a calibration tool between ammonite- and magnetostratigraphy: the Valanginian–Hauterivian transition, Geol. Carpath. 50 (1999) 91–96.
[39] M.A. Arthur, W.E. Dean, S.O. Schlanger, Variations in the global carbon cycle during the Cretaceous related to climate,

volcanism, and atmospheric CO_2, in: E.T. Sundquist, W.S. Broecker (Eds.), The Carbon Cycle and Atmospheric CO_2: Natural Variations Archean to Present, Am. Geophys. Union Mono., vol. 32, 1985, pp. 504–529.

[40] H.C. Jenkyns, Mesozoic anoxic events and palaeoclimate, Zentralbl. Geol. Paläontol. 1997 (1999) 943–949.

[41] H.C. Jenkyns, Evidence for rapid climate change in the Mesozoic–Palaeogene greenhouse world, Phil. Trans. R. Soc. (Lond.) A 361 (2003) 1885–1916.

[42] L.R. Kump, M.A. Arthur, Interpreting carbon–isotope excursions: carbonates and organic matter, Chem. Geol. 161 (1999) 181–198.

[43] J.P. Herbin, G. Deroo, J. Roucache, Organic geochemistry of lower Cretaceous sediments from Site 535, Leg 77: Florida Straits, Init. Rep. Deep Sea Drill. Proj. 77 (1983) 459–474.

[44] ODP Shipboard Scientific Party, Leg 198 Preliminary Report, Extreme Warmth in the Cretaceous and Paleogene: A Depth Transect on Shatsky Rise, Central Pacific, 2002, pp. 1–165.

[45] G.E. Claypool, J.P. Baysinger, Analysis of Organic matter in sediment cores from the Morrocan Basin, Deep Sea Drilling Project Sites 415 and 416, Init. Rep. Deep Sea Drill. Proj. 50 (1980) 605–608.

[46] R. Bersezio, E. Erba, M. Gorza, A. Riva, Berriasian–Aptian black shales of the Maiolica formation (Lombardian Basin, Southern Alps, Northern Italy): local to global events, Palaeogeogr. Palaeoclimatol. Palaeoecol. 180 (2002) 253–275.

[47] A.P. Menegatti, H. Weissert, R.S. Brown, R.V. Tyson, P. Farrimond, A. Strasser, M. Caron, High-resolution δ^{13}C stratigraphy through the Early Aptian "Livello Selli" of the Alpine Tethys, Paleoceanography 13 (1998) 530–545.

[48] S.P. Hesselbo, D.R. Gröcke, H.C. Jenkyns, C.J. Bjerrum, P.L. Farrimond, H.S. Morgans-Bell, O.R. Green, Massive dissociation of gas hydrate during a Jurassic oceanic anoxic event, Nature 406 (2000) 392–395.

[49] E. Erba, J.E.T. Channell, M. Claps, C. Jones, R. Larson, B. Opdyke, I.P. Silva, A. Riva, G. Salvini, S. Torricelli, Integrated stratigraphy of the Cismon APTICORE (Southern Alps, Italy): a "reference section" for the Barremian–Aptian interval at low latitudes, J. Foram. Res. 29 (1999) 371–391.

[50] U.G. Wortmann, H. Weissert, Timing platform drowning to perturbations of the global carbon cycle with a δ^{13}Corg-curve from the Valanginian of DSDP Site 416, Terra Nova 12 (2000) 289–294.

[51] A. Ando, T. Kakegawa, R. Takashima, T. Saito, New perspective on Aptian carbon isotope stratigraphy: data from δ^{13}C records of terrestrial organic matter, Geology 30 (2002) 227–230.

[52] U. Heimhofer, P.A. Hochuli, S. Burla, N. Andersen, H. Weissert, Terrestrial carbon–isotope records from coastal deposits (Algarve, Portugal): a tool for chemostratigraphic correlation on an intrabasinal and global scale, Terra Nova 15 (2003) 8–13.

[53] T. Hasegawa, Cenomanian–Turonian carbon isotope events recorded in terrestrial organic matter from northern Japan, Palaeogeogr. Palaeoclimatol. Palaeoecol. 130 (1997) 251–273.

[54] T. Hasegawa, L.M. Pratt, H. Maeda, Y. Shigeta, T. Okamoto, T. Kase, K. Uemura, Upper Cretaceous stable carbon isotope stratigraphy of terrestrial organic matter from Sakhalin, Russian Far East: a proxy for the isotopic composition of paleoatmospheric CO_2, Palaeogeogr. Palaeoclimatol. Palaeoecol. 189 (2003) 97–115.

[55] S.A. Robinson, S.P. Hesselbo, Fossil-wood carbon-isotope stratigraphy of the non-marine Wealden Group (Lower Cretaceous, southern England), J. Geol. Soc. (Lond.) 161 (2004) 133–145.

[56] D.R. Gröcke, Carbon–isotope stratigraphy of terrestrial plant fragments in the Early Cretaceous from south-eastern Australia, in: D.L. Wolberg, E. Stump, G.R. Rosenberg (Eds.), Dinofest™ International, The Academy of Natural Sciences, Philadelphia, 1997, pp. 457–461.

[57] D.R. Gröcke, Carbon–isotope analyses of fossil plants as a chemostratigraphic and palaeoenvironmental tool, Lethaia 31 (1998) 1–13.

[58] D.R. Gröcke, S.P. Hesselbo, H.C. Jenkyns, Carbon–isotope composition of Lower Cretaceous fossil wood: ocean-atmosphere chemistry and relation to sea-level change, Geology 27 (1999) 155–158.

[59] J.C. McElwain, D.J. Beerling, F.I. Woodward, Fossil plants and global warming at the Triassic–Jurassic boundary, Science 285 (1999) 1386–1390.

[60] S.P. Hesselbo, S.A. Robinson, F. Surlyk, S. Piasecki, Terrestrial and marine extinction at the Triassic–Jurassic boundary synchronized with major carbon cycle perturbation: a link to initiation of massive volcanism? Geology 30 (2002) 251–254.

[61] S.P. Hesselbo, H.S. Morgan-Bells, J.C. McElwain, P. McAllister Rees, S.A. Robinson, C.E. Ross, Carbon-cycle perturbation in the Middle Jurassic and accompanying changes in the terrestrial paleoenvironment, J. Geol. 111 (2003) 259–276.

[62] A.H. Jahren, N.C. Arens, G. Sarimiento, J. Guerrero, R. Amundson, Terrestrial record of methane hydrate dissociation in the Early Cretaceous, Geology 29 (2001) 159–162.

[63] E. Erba, A. Bartolini, R.L. Larson, Valanginian Weissert oceanic anoxic event, Geology 32 (2004) 149–152.

[64] E. Erba, F. Tremolada, Nannofossil carbonate fluxes during the Early Cretaceous: Phytoplankton response to nutrification episodes, atmospheric CO_2, and anoxia, Paleoceanography 19 (2004), doi:10.1029/2003PA000884.

[65] E.Y. Baraboshkin, B.T. Yanin, Korreliatziya valanzhinskikh otlozhenii Yugo-Zapadnogo i Tzentralnogo Kryma [The correlation of the Valanginian of the South-Western and Central Crimea], in: E.E. Milanovsky (Ed.), Ocherki po Geologii Kryma, Izdanie Geologicheskogo Faculteta Moskovskogo Gosudarstvennogo Universiteta, 1997, pp. 4–26 (in Russian).

[66] A. Ruffell, R. Evans, J.M. McKinley, Distinguishing faults from flooding surfaces on spectral gamma-ray logs, Am. Assoc. Pet. Geol. 88 (2004) 1–16.

[67] E.Y. Baraboshkin, The Tethyan/Boreal Problem as the result of paleobiogeographical changes: Early Cretaceous examples from the Russian Platform, Miner. Slov. 29 (1997) 250–252.

[68] V.V. Arkadiev, A.A. Atabekian, E.Y. Baraboshkin, T.N. Bogdanova, Stratigraphy and ammonites of Cretaceous deposits of South-West Crimea, Palaeontogr. Abt. A 255 (2000) 85–128.

[69] E.Y. Baraboshkin, I.A. Mikhailova, New and poorly known Valanginian ammonites from South-West Crimea, Bull. Inst. R. Sci. Nat. Belg., Sci. Terre. 70 (2000) 89–120.

[70] P.J. Hoedemaeker, M. Company, M.B. Aguirre-Urretta, E. Avrame, T.N.L. Bogdanova, L. Bujtor, F. Cecca, G. Delanoy, M. Ettachfini, L. Memmi, H.G. Owen, P.F. Rawson, J. Sandoval, J.M. Tavera, J.P. Thieuloy, S.Z. Tovbina, A. Vasicek, Ammonite zonation for the Lower Cretaceous of the Mediterranean region, basis for stratigraphic correlations within IGCP Project 262, Rev. Esp. Paleontol. 8 (1993) 117–120.

[71] S. Reboulet, F. Atrops, Comments and proposals about the Valanginian–Lower Hauterivian ammonite zonation of south-eastern France, Eclogae Geol. Helv. 92 (1999) 183–197.

[72] E.Y. Baraboshkin, A.S. Alekseev, L.F. Kopaevich, Cretaceous palaeogeography of the North-Eastern Peri-Tethys, Palaeogeogr. Palaeoclimatol. Palaeoecol. 196 (2003) 177–208.
[73] H. Weissert, A. Lini, K.B. Föllmi, O. Kuhn, Correlation of Early carbon isotope stratigraphy and platform drowning events: a possible link, Palaeogeogr. Palaeoclimatol. Palaeocol. 137 (1998) 189–203.
[74] J.E.T. Channell, F. Cecca, E. Erba, Correlations of Hauterivian and Barremian (Early Cretaceous) stage boundaries to polarity chrons, Earth Planet. Sci. Lett. 134 (1995) 125–140.
[75] O.B. Yampolskaya, E.J. Baraboshkin, A.Yu. Guzhikov, M.V. Pimenov, A.S. Nikulshin, Paleomagnetic section of Lower Cretaceous of Southwest Crimea. Vestnik Moskovskogo Universiteta. Geologiya, in press.
[76] R.R. Bidigare, A. Fluegge, K.H. Freeman, K.L. Hanson, J.M. Hayes, D. Hollander, J.P. Jasper, L.L. King, E.A. Laws, J. Milder, F.J. Millero, R. Pancost, B.N. Popp, P.A. Steinberg, S.G. Wakeham, Consistent fractionation of 13C in nature and in the laboratory: growth-rate effects in some haptophyte algae, Glob. Biogeochem. Cycles 11 (1997) 279–292.
[77] D.R. Gröcke, The carbon isotope composition of ancient CO_2 based on higher-plant organic matter, Phil. Trans. Roy. Soc. London Series A 360 (2002) 633–658.
[78] T. Hasegawa, Cretaceous terrestrial paleoenvironments of northeastern Asia suggested from carbon isotope stratigraphy: increased atmospheric $p$$CO_2$-induced climate, J. Asian Earth Sci. 21 (2003) 849–859.
[79] Ch. Körner, G.D. Farquhar, Z. Roksandic, A global survey of carbon isotope discrimination in plants from high latitudes, Oecologia 74 (1988) 623–632.
[80] P.K. van de Water, S.W. Leavitt, J.L. Betancourt, Trends in stomatal density and $^{13}C/^{12}C$ ratios of *Pinus flexilis* needles during last glacial–interglacial cycle, Science 264 (1994) 239–243.
[81] M.M.M. Kuypers, R.D. Pancost, J.S. Sinninghe-Damsté, A large and abrupt fall in atmospheric CO_2 concentration during Cretaceous times, Nature 399 (1999) 342–345.
[82] H.C. Jenkyns, Cretaceous anoxic events: from continents to oceans, J. Geol. Soc. London 137 (1980) 171–188.
[83] H. Leereveld, Upper Tithonian–Valanginian (Upper Jurassic–Lower Cretaceous) dinoflagellate cyst stratigraphy of the western Mediterranean, Cretac. Res. 18 (1997) 385–420.
[84] M. Melinte, J. Mutterlose, A Valanginian (Early Cretaceous) ''Boreal nannoplankton excursion" in sections from Romania, Mar. Micropal. 43 (2001) 1–25.
[85] E. Pucéat, C. Lécuyer, S.M.F. Sheppard, G. Dromart, S. Reboulet, P. Grandjean, Thermal evolution of Cretaceous Tethyan marine waters inferred from oxygen isotope composition of fish tooth enamels, Paleoceanography 18 (2003) 1029–1041.
[86] C. Dessert, B. Dupré, J. Gaillardet, L.M. François, C.J. Allègre, Basalt weathering laws and the impact of basalt weathering on the global carbon cycle, Chem. Geol. 202 (2003) 257–273.
[87] R.A. Berner, Z. Kothavala, Geocarb III: a revised model of atmospheric CO_2 over Phanerozoic time, Am. J. Sci. 301 (2000) 182–204.
[88] C.J. Poulsen, E.J. Barron, M.A. Arthur, W.H. Peterson, Response of the mid-Cretaceous global oceanic circulation to tectonic and CO_2 forcings, Paleoceanography 16 (2001) 1–17.
[89] H. Weissert, A. Lini, Ice Age interludes during the time of Cretaceous greenhouse climate, in: D.H. Muller, J.A. McKenzie, H. Weissert (Eds.), Controversies in Modern Geology, Academic Press, London, 1991, pp. 173–191.
[90] A.S. Gale, J. Hardenbol, B. Hathway, W.J. Kennedy, J.R. Young, V. Phansalkar, Global correlation of Cenomanian (Upper Cretaceous) sequences: evidence for Milankovitch control on sea level, Geology 30 (2002) 291–294.
[91] J.W. Patton, P.W. Choquette, G.K. Guennei, A.J. Kaltenback, A. Moore, Organic geochemistry and sedimentology of the Lower to mid-Cretaceous deep-sea carbonates, Sites 535 and 540, Leg 77, Int. Rep. Deep Sea Drill. Proj. 77 (1984) 417–443.
[92] P.J. Hoedemaeker, S. Reboulet, M.B. Aguirre-Urreta, P. Alsen, M. Aoutem, F. Atrops, R. Barragan, M. Company, C.G. Arreola, J. Klein, A. Lukeneder, I. Ploch, N. Raisossadat, P.F. Rawson, P. Ropolo, Z. Vasícek, M.G.E. Wippich, Report on the 1st International Workshop of the IUGS Lower Cretaceous Ammonite Working Group, the 'Kilian Group' (Lyon, 11 July 2002), Cretac. Res. 24 (2003) 89–94.
[93] J.E.T. Channell, T.J. Bralower, P. Grandesso, Biostratigraphic correlation of Mesozoic polarity chrons CM1 to CM23 at Capriola and Xausa (Southern Alps, Italy), Earth Planet. Sci. Lett. 85 (1987) 203–221.
[94] J.E.T. Channell, E. Erba, M. Nakanishi, K. Tamaki, Late Jurassic–Early Cretaceous time scales and oceanic magnetic anomaly block models, in: W.A. Berggren, M.-P. Aubry, J. Hardenbol (Eds.), Geochrononology, Time Scales and Global Stratigraphic Correlation, SEPM Spec. Publ, vol. 54, 1995, pp. 51–63.